A Novel Framework to Automatically Fuse Multi-platform Lidar Data in Forest Environments Based on Tree Locations

Hongcan Guan, Yanjun Su, Tianyu Hu, Rui Wang, Qin Ma, Qiuli Yang, Xiliang Sun, Yumei Li, Shichao Jin, Jing Zhang, Qin Ma, Min Liu, Fayun Wu, Qinghua Guo

***Abstract*—The emerging near-surface light detection and ranging (lidar) platforms (e.g., terrestrial, backpack, mobile and unmanned aerial vehicle/UAV) have shown great potential for forest inventory. However, different lidar platforms have limitations either in data coverage or in capturing under-canopy information. The fusion of multi-platform lidar data is a potential solution to this problem. Due to the complexity and irregularity of forests and the inaccurate positioning information under forest canopies, current multi-platform data fusion still involves substantial manual efforts. In this study, we proposed an automatic multi-platform lidar data registration framework based on the assumption that each forest has a unique tree distribution pattern. Five steps are included in the proposed framework, i.e. individual tree segmentation, triangulated irregular network (TIN) generation, TIN matching, coarse registration, and fine registration. TIN matching, as the essential step to find corresponding tree pairs from multi-platform lidar data, uses a voting strategy based on the similarity of triangles composed of individual tree locations. The proposed framework was validated by fusing backpack and UAV lidar data and fusing multi-scan terrestrial lidar data in coniferous forests. The results showed that both registration experiments could reach a satisfying data registration accuracy (horizontal RMSE <30 cm, vertical RMSE <20 cm). Moreover, the proposed framework was insensitive to individual tree segmentation errors, when the individual tree segmentation accuracy was higher than 80%. We believe that the proposed framework has the potential to increase the efficiency of accurately registering multi-platform lidar data in forest environments.**

***Index Terms*—multi-platform lidar, tree location, registration, forest**

I. Introduction

Light detection and ranging (lidar) can be used to accurately estimate forest structure attributes (e.g., tree height, diameter at breast height/DBH, canopy cover, leaf area index, crown base height) from its rich three-dimensional (3D) information [1]. It has been proven to be a highly useful remote sensing technique in the practices of forest inventory [2]-[4] and forest management [5]-[7]. Currently, airborne, unmanned aerial vehicle (UAV)-borne, mobile, and terrestrial lidar systems are the most commonly used lidar platforms in forest-related applications [8]-[11]. However, each of these lidar platforms has its own limitations. The down-looking airborne and UAV-borne lidar systems can provide highly accurate tree canopy information, but lack tree trunk information [12]; mobile lidar systems (e.g., backpack lidar) can provide detailed tree trunk information, but the limited vertical field of view and measurement range may result in the missing of upper canopy information [13]; single-location scans of terrestrial laser scanning (TLS) suffer from the occlusion effect of branches and leaves, and the registration of multi-scan TLS data can be highly time-consuming [14], [15]. The fusion of multi-platform lidar data has the potential to provide an ultimate solution to address the limitations of each lidar platform.

Currently, there are three commonly used point cloud registration frameworks, including target-based methods, feature-based methods, and point-based methods [16]-[18]. Target-based methods usually need the assistance of exterior information to register lidar point clouds, e.g., positioning information from a global positioning system (GPS) [19], registration targets that can be easily identified [20], [21], or color information provided by cameras [22], [23]. Feature-based methods work similarly to target-based methods, which use tie points/lines/polygons to register lidar point clouds, but these features are identified within lidar point clouds (e.g., buildings, roofs, roads and traffic signs) [24]. Point-based

This work was supported by the National Key R&D Program of China (2016YFC0500202), the Key Research Program of the Chinese Academy of Science (KFZD-SW-319-06), National Natural Science Foundation of China (41871332), the "Study on Monitoring of the Program for Targeted Improvement of Forest Quality" project (0011107), the CAS Pioneer Hundred Talents Program. (*Corresponding author: Yanjun Su.*)

H. Guan, Y. Su, T. Hu, R. Wang, Q. Ma, Q. Yang, X. Sun, Y. Li, S. Jin, J. Zhang and Q. Guo are with the State Key Laboratory of Vegetation and Environmental Change, Institute of Botany, Chinese Academy of Sciences, Beijing 100093, China, and also with the University of Chinese Academy of Sciences, Beijing 100049, China. (e-mail: guanhongcan@gmail.com; suyanjun1987@gmail.com; tianyuhu@ibcas.ac.cn; wangrui@ibcas.ac.cn; maqin@ibcas.ac.cn; yangqiuli621@gmail.com; sxl456852@ibcas.ac.cn; ai10056@126.com; jinshichao1993@gmail.com; eve.zhangj@gmail.com; guo.qinghua@gmail.com).

Q. Ma is with the Department of Forestry, Mississippi State University, Mississippi State, MS, 39762, United States. (e-mail: qm153@msstate.edu).

M. Liu is with the China National Forestry Economics and Development Research Center, National Forestry and Grassland Administration, Beijing 100714, China. (e-mail: rdlmin@aliyun.com).

F. Wu is with the Academy of Inventory and Planning, National Forestry and Grassland Administration, Beijing 100714, China. (e-mail: wufayun@sina.com).

methods directly match lidar point clouds based on the geometric information provided by lidar points, and the iterative closest point (ICP) algorithm is one of the most widely used methods under this category [25], [26]. However, point cloud registration frameworks are typically problematic in forested scenes. The exterior registration information required by the target-based methods is either unavailable, inaccurate or hard to acquire in forests. For example, GPS positioning information might become unreliable under forest canopies because of multipath errors and the attenuation of GPS signals [27]. Further, arranging ground targets or acquiring color imagery can be very time-consuming and expensive [28]. Feature-based methods are widely used in indoor and urban environments, where regular features (e.g., parallel and orthogonal line segments [29], [30] and conjugate least-squares surfaces [31], [32]) can be easily found. Forest environments have much higher complexity and irregularity than indoor and urban environments, and similar regular features as in indoor and urban environments can be hardly found or might be completely absent. Point-based methods, such as ICP, usually require the lidar point clouds to be coarsely registered before running the algorithm. However, such coarse registration in forest environments is usually achieved by manually selecting tie points, which is a labor-intensive and time-consuming process.

Recently, marker-free data fusion solutions have been proposed to overcome the issues of missing referencing features in forests. For example, Henning *et al.* [33] and Liu *et al.* [34] proposed to use geometric features within the lidar point clouds (e.g., stem centers and stem curves) to register multi-scan TLS data; Kelbe *et al.* [35] proposed a multi-scan TLS data registration method through the use of populated triplet sets of DBHs, tree locations, and eigenvalues; Polewski et al. [36] used simulated annealing to find the optimal 3D transformation between the respective coordinate systems of two tree location sets derived from backpack and UAV lidar data. These methods either rely on tree stem geometric information or look for a globally optimized registration solution using constraints of tree attributes such as DBHs and tree locations. However, tree stem geometric information is unavailable in top-view lidar data (e.g., UAV lidar data), and globally optimized solutions might fail when the estimation accuracies of tree attributes are low. How to accurately and efficiently register multi-platform lidar point clouds in forested scenes is still a big challenge in lidar forest applications.

In this study, we propose a novel multi-platform lidar data registration framework for forest applications based on the unique spatial distribution of trees in a forest stand, with tree pairs identified from multi-platform lidar data as the only required features in the registration process. This paper is organized as follows. Sections II introduces the methodology of the proposed data registration framework, Section III describes the experimental design and results for evaluating the proposed framework, Section IV discusses the robustness and limitations of the proposed framework and Section V gives the conclusion.

II. Methodology

The proposed framework includes five steps, i.e., individual tree segmentation, triangulated irregular network (TIN) generation, TIN matching, coarse registration, and fine registration (Fig. 1). The detailed information of each step is presented in the following sections.

A. Individual Tree Segmentation

Extracting individual tree locations is the pre-requisite of the proposed point cloud registration framework. Individual tree segmentation is a point cloud processing step that can automatically identify individual tree locations from lidar point clouds. There have been numerous individual tree segmentation algorithms proposed in the literature, which can be generally divided into two groups: canopy height model (CHM) segmentation [37]-[39] and point cloud segmentation (PCS) [40]-[42]. Lidar data acquired from different platforms and forest conditions usually require different segmentation schemes to obtain optimized segmentation results. Jakubowski *et al.* [43] made a comprehensive comparison of the performance of CHM segmentation and PCS under different forest conditions. The individual tree segmentation method should be chosen based on the data acquisition platform and forest conditions. The output individual tree coordinates (i.e., *X*, *Y* and *Z*) can be used as the input of the proposed framework. The *Z* coordinate of each tree is represented by the elevation of the tree base. In this study, we used the mean elevation of all ground points within a 1 m buffer to represent the *Z* coordinate so that the influence of different tree position definitions from different platforms (e.g., treetop from UAV-borne lidar and tree base from terrestrial lidar) can be minimized.

B. TIN Generation

This study assumes that every forest stand should have a unique spatial distribution of trees and this spatial pattern should not change in a short time period within which multiple lidar data sets are acquired. In other words, the spatial relationship between each tree and its neighboring trees should be constant. To identify the spatial pattern of tree distributions, the plane coordinates (i.e., *X* and *Y*) of each individual tree and its neighboring trees are transformed to a simple geometric feature by constructing a TIN using the Delaunay triangulation [44]. Based on the above-mentioned assumptions, a particular tree identified from different lidar platforms should form a similar TIN with its defined neighbors. Therefore, we should be able to find corresponding tree pairs by matching the TINs generated from different lidar platforms.

In the process of TIN generation, each tree location is considered as a search point and its neighboring tree locations can be found by the k-nearest neighbor search method. Moreover, in order to avoid ambiguous TINs, the search point does not participate in the TIN generation. For example, as

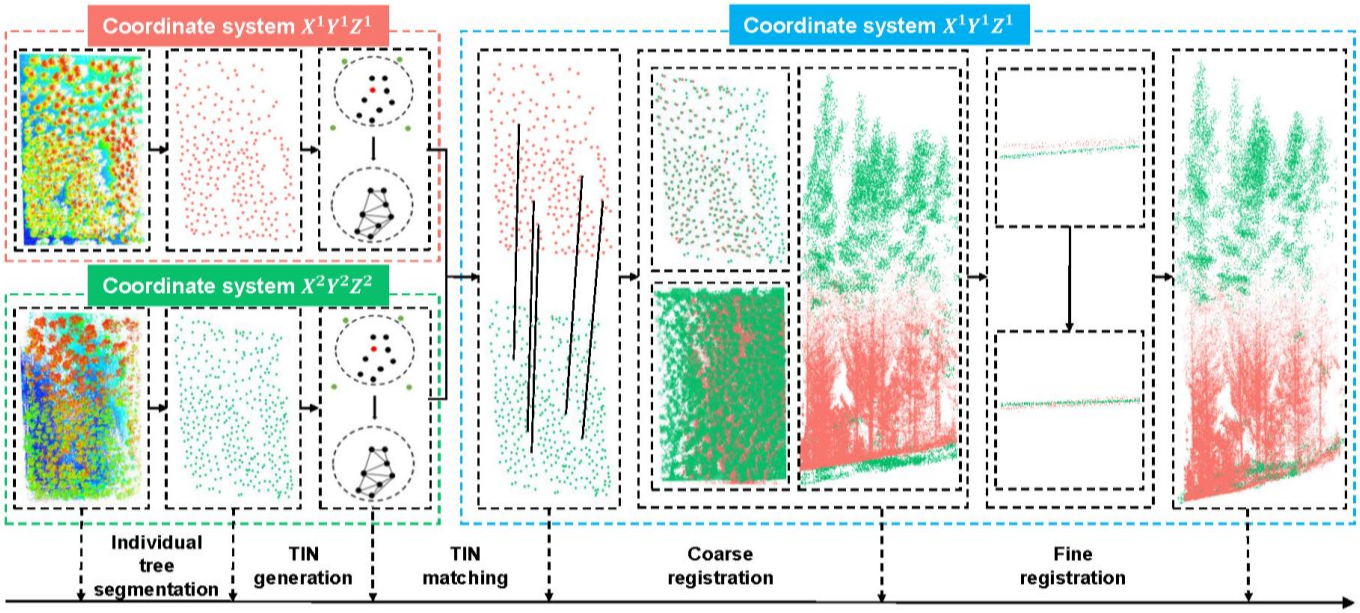

Fig. 1. The five-step process of the proposed multi-platform lidar registration framework. Red points represent the lidar data acquired from the side view backpack lidar, and green points represent the vertical UAV lidar data.

shown in Fig. 2, the three search points have the same search neighbors. In the case of TIN generation including the search point itself, the generated TINs would be the same; if the search point is excluded, the generated TINs would be distinctive from each other. Two sets of TINs generated from segmented trees in multi-platform lidar data are represented as $TIN^1 = \{TIN_1^1, TIN_2^1, \ldots, TIN_k^1\}$ and $TIN^2 = \{TIN_1^2, TIN_2^2, \ldots, TIN_l^2\}$, where k and l are the numbers of trees derived from two lidar datasets, respectively.

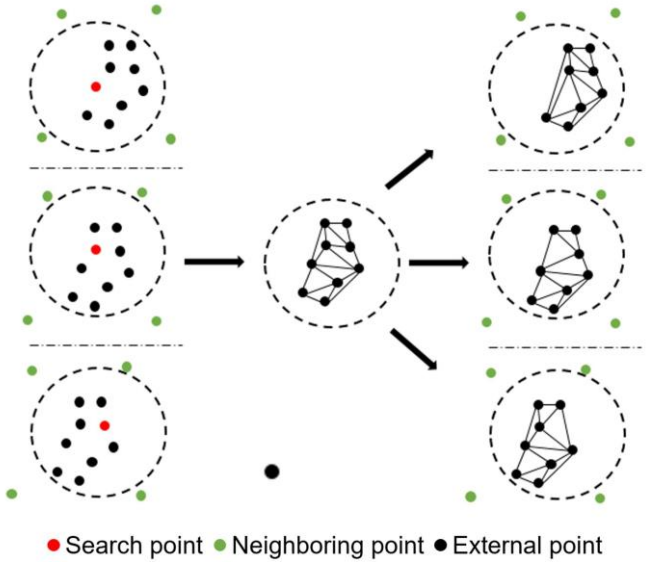

Fig. 2. An illustration of the TIN generation and ambiguous TIN elimination for tree locations using a point cloud from one platform.

C. TIN Matching

The plane coordinates (i.e., X and Y) of the same trees obtained by the individual tree segmentation from different lidar data can be slightly different. For example, the individual tree locations obtained from UAV-borne lidar data are centers of tree crowns; while the individual tree locations obtained from mobile and terrestrial lidar data are the centers of tree bases. Meanwhile, the incomplete point cloud of trees and the dense tree distribution can bring many undetected and falsely detected trees in segmentation. These errors caused by individual tree segmentation from different lidar data may bring failures in the tree matching process if very strict rules were used. Therefore, a tolerant matching method should be used to match TINs. To avoid falsely matched TINs during the tolerant matching process, the matched TINs are further filtered by using a random sample consensus (RANSAC)-based method.

During the tolerant matching process, a voting strategy is used to count the number of similar triangles between two TINs and find the best matched TIN pairs iteratively. Each TIN in TIN^1 is compared with all TINs in TIN^2 to calculate the matching scores based on the similarities among the triangles within each TIN pair. The similarity of triangles is evaluated by two parameters, the area similarity S and the angle similarity I. Assuming that $Tri_p^{i,1}$ is the p^{th} triangle in TIN_i^1, and $Tri_q^{j,2}$ is the q^{th} triangle in TIN_j^2, the area similarity S can be calculated from the following equation,

$$S = 1 - \frac{|l_a l_b \sin C - l'_a l'_b \sin C'|}{\frac{l_a l_b \sin C + l'_a l'_b \sin C'}{2}} \quad (1)$$

where l_a and l_b are two sides of $Tri_p^{i,1}$, l'_a and l'_b are two sides of $Tri_q^{j,2}$, and C and C' are the angles between l_a and l_b and between l'_a and l'_b, respectively. The triangle pair $Tri_p^{i,1}$ and $Tri_q^{j,2}$ has three angle similarity components, i.e., I_A, I_B, and I_C, where A, B and C are the three angles of $Tri_p^{i,1}$. Zhou *et al.* [45] proposed the criteria of calculating angle similarity based on the Gaussian distribution. Taking I_C as an example, the angle similarity I_C between C and C' can be calculated as,

$$I_C = cos^3(\frac{\pi}{2}(1-u(C))) \quad (2)$$

$$u(C) = e^{-\frac{1}{2\sigma^2}(C-C')^2} \quad (3)$$

where $\sigma = C/6$. The final angle similarity I is calculated as the average of the three angle similarity components,

$$I = (I_A + I_B + I_C)/3 \quad (4)$$

The overall similarity OS between the triangle pair $Tri_p^{i,1}$ and $Tri_q^{j,2}$ is calculated as,

$$OS = (I + S)/2 \quad (5)$$

Note that if I or S was smaller than the user-defined thresholds T_I or T_S, the OS value should be set to zero instead of being calculated from Eq. 5. By iterating the calculation between all triangle combinations, an OS matrix (OSM) can be built as,

$$OSM = \begin{bmatrix} OS_{11} & OS_{12} & \cdots & OS_{1n} \\ OS_{21} & OS_{22} & \cdots & OS_{2n} \\ \vdots & \vdots & \vdots & \vdots \\ OS_{m1} & OS_{m2} & \ldots & OS_{mn} \end{bmatrix} \quad (6)$$

where m and n are the number of triangles in TIN_i^1 and TIN_j^2, respectively.

The voting process for the TIN pair of TIN_i^1 and TIN_j^2 is shown in Fig. 3. Within OSM, the largest OS is first identified and marked, and all elements on the corresponding row and column of the matrix are set to zero. Then, the new largest OS excluding the previous largest OS is identified and marked, and all elements on the corresponding row and column of the matrix are set to zero. This process is repeated until all unmarked elements become zero. Each of the remaining marked elements is treated as an equal-weighted vote with a value of one, and the final vote score (VS) between TIN_i^1 and TIN_j^2 is calculated as the sum of all votes.

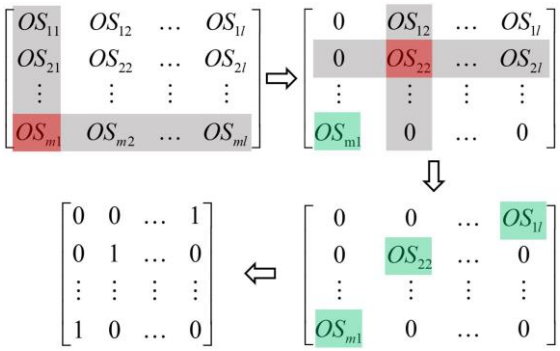

Fig. 3. An illustration of the voting process for TIN matching. Elements colored in green represent marked elements and elements colored in red represent the largest element excluding marked elements.

After calculating the VS between TIN_i^1 and all TINs in TIN^2, the TIN(s) with the largest VS is/are picked out. If the largest VS value is smaller than the user-defined voting score threshold T_{VS}, the search point in dataset 1 is treated as no matched tree location point can be found in dataset 2. If the largest VS value is larger than user-defined threshold T_{VS} and there is only one matched point in dataset 2, the search point in dataset 1 and the matched tree location point in dataset 2 are treated as a pair of trees. If the largest VS value is larger than user-defined threshold T_{VS} and there are more than one matched points in dataset 2, the thresholds T_I and T_S are iteratively increased to eliminate the one-to-many phenomenon using the following equations,

$$T_I^{'} = (1-f)T_I \times 1.1^N \quad (7)$$

$$T_s^{'} = (1-f)T_s \times 1.1^N \quad (8)$$

$$f = \frac{p_{l_{max}} - 50}{50} \times 10\% \quad (9)$$

where N is the number of iterations which should be smaller than the user-defined maximum number of iterations T_N, and $p_{l_{max}}$ is the percentile of the maximum side in a triangle among all sides of triangles of the whole study area. Since $p_{l_{max}}$ is between 0 and 100, the scale factor f should be in the range of [-0.1, 0.1]. The scale factor f here is used to give looser thresholds in areas with sparse trees, and give stricter thresholds in areas with dense trees, because the individual tree segmentation error is higher in areas with dense trees.

The whole TIN matching process can be described as the following pseudo codes.

```
For i = 1 to k
    Generate TIN_i^1 from the neighbors of the search tree point i
    For j = 1 to l
        Generate TIN_j^2 from the neighbors of the search tree point j
        For p = 1 to m
            For q= 1 to n
                Calculate S and I between Tri_p^{i,1} and Tri_q^{j,2}
                If S ≥ T_S and I ≥ T_I
                    OSM(p, q) = (S+I)/2
                Else
                    OSM(p, q) = 0
            End for
        End for
        Do when all unmarked elements in OSM are not 0
            Find and mark the largest unmarked OSM(row, col)
            Set unmarked OSM(row, :) and OSM(:, col) as 0
        End do
        VS(i, j) = the number of marked elements in OSM
    End for
    If max(VS(i, :)) < T_VS
        There is no matched tree location point for i
    Else if max(VS(i, :)) ≥ T_VS and count(max(VS(i, :))) == 1
        The matched tree point in TIN^2 for tree location point i is found
    Else if max(VS(i, :)) ≥ T_VS and count(max(VS(i, :))) > 1
        Updating the thresholds T_I and T_S and iterate the TIN matching process
        until count (max(VS(i, :))) == 1 or the number of iterations > T_N
End For
```

From the above process, a set of tree location pairs can be collected from two lidar datasets from different platforms. The number of matched tree pairs is usually much higher than the required number of tree pairs for performing coarse registration. To ensure the coarse registration quality, the matched tree pairs are filtered and optimized by the RANSAC algorithm [46], [47], using the OpenCV implementations with default parameters.

D. Coarse Registration

The matched tree pairs are acquired through the TIN matching of plane coordinates (i.e., *X* and *Y*), while the 3D coordinates (i.e., *X*, *Y* and *Z*) of matched tree pairs from multi-platform lidar data are used to calculate the rotation matrix and translation vector to transform the target point cloud to the source point cloud. Considering the fact that the distance measurements from different lidar platforms are all highly accurate [48], it is reasonable to set the scale factor of the rotation matrix as 1. Therefore, the coarse registration process can be expressed as,

$$\begin{bmatrix} X \\ Y \\ Z \end{bmatrix} = R \begin{bmatrix} X' \\ Y' \\ Z' \end{bmatrix} + T \tag{10}$$

where X, Y and Z are the coordinates of the source point cloud, X', Y' and Z' are the coordinates of the target point cloud, and R and T are the rotation matrix and translation vector, respectively.

E. Fine Registration

In the fine registration step, the ICP algorithm, a point-based matching method based on minimizing the cumulative distance between two point clouds [49], is used to further improve the multi-platform lidar data registration accuracy. To reduce the chance of mismatching errors in ICP results, the ICP algorithm should be performed on the overlapped areas of different lidar datasets with distinct characteristics. For example, if two multi-platform lidar datasets share a large portion of ground points and the ground is a rugged terrain, their ground points can be selected to run the ICP algorithm; if two multi-platform lidar datasets share a large portion of tree trunks, their point clouds within the height range of tree trunks can be selected to run the ICP algorithm.

III. Experimental analysis

A. Study Area and Data Collection

The study area is located in the Mulan Paddock, Hebei Province, China (42.12 °N, 117.35 °E). It is a planted forest and the dominant tree species are Pinus sylvestris var. mongolica Litv. and Pinus tabuliformis Carrière. Three study sites were selected within the study area. Site 1 has an area of 7,890 m^2 with an 8 m elevation variation, site 2 has an area of 5,814 m^2 with a 46 m elevation variation, and site 3 has an area of 1,885 m^2 with a 3 m elevation variation. The average canopy cover is 71%, 46%, and 65% in site 1, site 2 and site 3, the average tree height is 18 m, 17 m and 20 m, and the average tree density is 283 trees/ha, 275 trees/ha and 1,056 trees/ha. Three widely used lidar platforms, including a backpack lidar platform, a UAV-borne lidar platform, and a TLS platform, were used to collect multi-platform lidar data within the three study sites in August 2018. Their hardware models and specifications are listed in Table I. The UAV lidar system (Green Valley International LiAir 200) integrates a HESAI Pandar40 laser scanner and a high-precision inertial navigation system, whose relative positioning accuracy is specified as ±5 cm. The backpack lidar system (Green Valley International LiBackpack 50) is equipped with a Velodyne Puck VLP-16 laser scanner, and its relative positioning accuracy is specified as ±5 cm. The Riegl VZ-400i is a high-precision TLS scanner, and its measurement accuracy is ±0.5 cm. Sites 1 and 2 were covered by both UAV and backpack lidar data. The UAV lidar data in site 1 and site 2 were collected from a single flight line and two flight lines, respectively. The flight attitude was about 150 m above ground at both study sites, and the overlap ratio between flight lines in site 2 was about 50%. The point density of the collected UAV lidar data is about 158 pts/m^2 in site 1 and 238 pts/m^2 in site 2 (Fig. 4b and c). The backpack lidar data at study sites 1 and 2 were all collected following a "S"-shape trajectory with a ~10m horizontal spacing. The collected backpack lidar data had an average point density of 2,042 pts/m^2 in site 1 and 2,092 pts/m^2 in site 2 (Fig. 4b and c). It should be noted that the extents of UAV lidar data were slightly larger than those of backpack lidar data to ensure that they fully covered the backpack data. Site 3 was only covered by TLS data. The Riegl VZ-400i scanner was used to cover the study area using four separate scans. The distance between the scan position 1 and scan position 2, 3 and 4 was about 13 m, 15 m and 20 m, while the overlap ratio was about 51%, 40% and 33%, respectively. Six high-reflectance targets were installed in site 3, and they were used to manually register the TLS scans using the Riegl RiSCAN Pro software. In order to reduce the errors of individual tree segmentation caused by incomplete scan of trees, we used a rectangle with a size of 25 m × 25 m to clip the original TLS data of each scan. The average point density of each TLS scan was about 22,167 pts/m^2 (Fig. 4b and c).

In study sites 1 and 2, we put a 60 cm × 90 cm referencing standard white board in an open area so that it could be seen by both the backpack lidar and UAV lidar (Fig. 5a). The referencing white board was used to evaluate the relative positioning accuracy of the collected backpack and UAV lidar data (Fig. 5b and c). By fitting a plane from the points falling on the referencing white board, the distance between each point and the fitted plane was calculated. The relative positioning accuracy was calculated as the root-mean-square error (RMSE) of these points to the fitted plane. As can be seen in Fig. 6, the backpack and UAV lidar data at both sites had a relative positioning error lower than 10 cm, which agreed with the nominal specifications from the manufacturer. The referencing white board was also used to evaluate the multi-platform lidar data registration accuracy in the following experiment.

TABLE I
SPECIFICATIONS OF THE THREE LIDAR PLATFORMS USED IN THIS STUDY

	UAV	**Backpack**	**Terrestrial**
Sensor	HESAI Pandar40 (GreenValley LiAir 200)	Velodyne Puck VLP-16 (GreenValley LiBackpack 50)	VZ-400i (Riegl)
Scan range	0.3-200 m	100 m	400 m
Relative accuracy	±5 cm	±5 cm	±0.5 cm
Pulse repetition rate	720 KHz	300 KHz	122 KHz

Angular resolution (Vertical)	0.33°	2 °	better 0.005°
Angular resolution (Horizontal)	0.2°	0.1 °– 0.4 °	better 0.005°

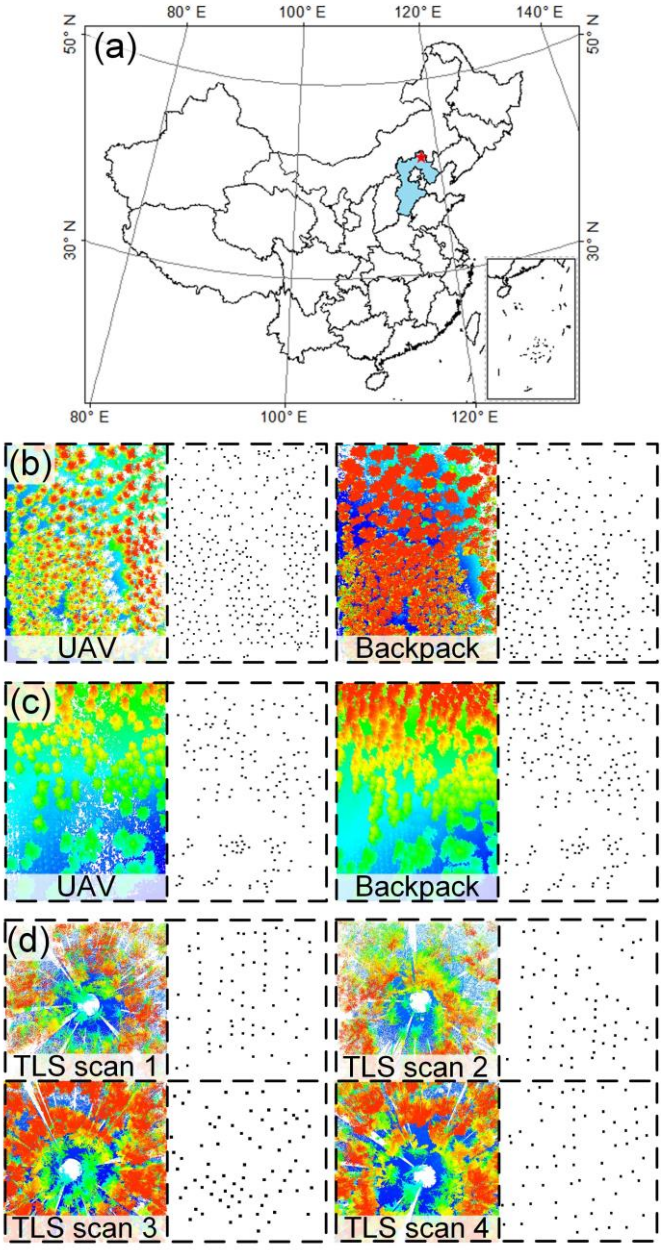

Fig. 4. (a) The location of the study area; (b) the collected UAV (left panel) and backpack (right panel) lidar data in study site 1, and their corresponding individual tree segmentation results (black dots); (c) the collected UAV (left panel) and backpack (right panel) lidar data in study site 2, and their corresponding individual tree segmentation results (black dots); and (d) the collected four TLS scans in study site 3, and their corresponding individual tree segmentation results (black dots).

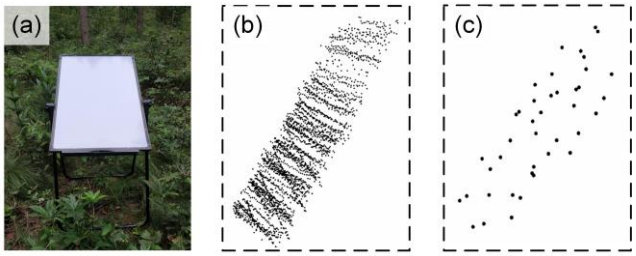

Fig. 5. An example of (a) the setup of the referencing standard white board, and its corresponding point clouds obtained from (b) backpack lidar and (c) UAV lidar systems.

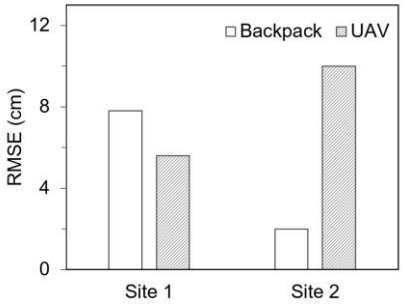

Fig. 6. The relative positioning accuracy of the collected backpack lidar data and UAV lidar data at the two study sites.

B. *Experiment Design*

1) Data Processing: It is inevitable to have noise in the collected lidar data due to factors such as tree movement with winds and flying birds. In this study, we used the outlier removal tool integrated in the GreenValley International LiDAR360 software (https://greenvalleyintl.com/software) to remove noise points in all collected lidar data. All lidar data were filtered to classify ground points using the improved progressive triangulated irregular network densification filtering algorithm proposed by Zhao et al. [50], which has shown to be robust under different forest and terrain conditions. Finally, the obtained ground points were used to normalize the original lidar point clouds to produce the input data for individual tree segmentation by using the LiDAR360 software.

2) Individual Tree Segmentation: Different segmentation strategies were used to segment the UAV lidar data and the backpack and terrestrial lidar data. For the UAV lidar data, the top-down PCS algorithm proposed by Li *et al.* [40] was used to identify individual tree locations; and for the backpack and terrestrial lidar data, the bottom-up PCS algorithm proposed by Tao *et al.* [42] was used. These algorithms use a similar principle in the segmentation process, which first identifies seed points of individual trees and then labels other points by finding the shortest path to seed points using the comparative shortest-path algorithm. The difference is that the top-down PCS algorithm finds seed points by recognizing treetops, but the bottom-up PCS algorithm finds seed points by recognizing tree bases. The PCS methods were selected in this study because studies have shown that they outperformed CHM methods in coniferous forests and were less influenced by under-canopy low-vegetation points [43].

To evaluate the individual tree segmentation results, we visually counted the number of trees and marked their corresponding locations from the backpack or terrestrial lidar

data. Three accuracy statistics i.e., recall (r), precision (p), and F-score (F), were calculated by comparing with individual tree locations derived visually,

$$r = \frac{TP}{TP + FN} \quad (11)$$

$$p = \frac{TP}{TP + FP} \quad (12)$$

$$F = 2 \times \frac{r \times p}{r + p} \quad (13)$$

where true positive (TP) denotes the number of trees correctly detected, false negative (FN) denotes the number of trees that were not detected, and false positive (FP) denotes the number of trees falsely detected. r indicates the tree segmentation completeness, p indicates the correctness of the detected trees, and F is the overall accuracy taking both commission and omission errors into consideration. Note that the individual tree segmentation accuracies of the UAV and TLS lidar data were calculated from the corresponding post-registered datasets so that they could be compared with individual tree locations derived visually.

3) Multi-platform lidar data registration: Two experiments were conducted to evaluate the performance of the proposed multi-platform lidar data registration framework, i.e., the registration between backpack lidar data and UAV lidar data and the registration among multi-scan TLS data. There are overall five parameters in the proposed registration framework (Table II). Among these parameters, T_I and Ts are two iteratively increasing thresholds, which can be set to relatively small values as initial values, and T_N can be set to a relatively large value based on experience. The remaining two parameters NN and T_{VS} can be estimated using a trial and error method. A detailed discussion of the parameter setting will be described in the discussion section. The two experiments used the same set of parameter values without any changes. The only difference in the registration procedures of the two experiments was that the registration of backpack and UAV lidar data used ground points to perform the fine registration, while the registration of multi-scan terrestrial lidar data used all points. Moreover, for the registration of TLS data, we used the data from scan position 1 as the target data and the TLS data from scan positions 2, 3 and 4 as the source data to be aligned with the reference coordinate system.

TABLE II
A LIST OF PARAMETERS IN THE PROPOSED MULTI-PLATFORM LIDAR DATA REGISTRATION FRAMEWORK AND THEIR CORRESPONDING VALUES USED IN THIS STUDY.

Parameter	Description	Value
NN	The number of neighboring tree points used to build TIN	9
T_S	The initial threshold for area similarity	0.8
T_I	The initial threshold for angle similarity	0.7
T_{VS}	The threshold for voting score	5
T_N	The max number of iterations	3

4) Accuracy assessment: The registration accuracy of backpack and UAV lidar data was evaluated using the referencing white board. The backpack lidar points falling on the referencing white board were first used to fit a plane $Z=f(X,Y)$. Then, the horizontal and vertical distances of each transformed UAV lidar point falling on the referencing white board to the fitted plane were calculated, and the horizontal error E_H and vertical error E_V were calculated as,

$$E_H = \sqrt{\frac{\sum_{i=1}^{n}(X_i'Y_i' \to Z=f(X,Y))^2}{n}} \quad (14)$$

$$E_V = \sqrt{\frac{\sum_{i=1}^{n}(Z_i' \to Z=f(X,Y))^2}{n}} \quad (15)$$

where n is the number of UAV points falling on the referencing white board, and $X_i'Y_i' \to Z = f(X,Y)$ and $Z_i' \to Z = f(X,Y)$ represent the horizontal and vertical distances from a point to the fitted plane.

Since the installed referencing white board was not within the scanning area of TLS scans, the above accuracy assessment methods could not be used for the evaluation of multi-scan TLS data registration. Considering the high positioning accuracy of TLS data and the high overlap rate between TLS scans, registration accuracy of multi-scan TLS data was represented by the residual after running ICP. The obtained ICP residual value was compared with the manual registration residual obtained using the Riegl RiSCAN Pro software.

C. Backpack Lidar and UAV Lidar Registration Results

The individual tree segmentation results from the backpack and UAV lidar data in the two study sites were shown in Fig. 4b-e. Overall, the backpack lidar data allowed a very high individual tree segmentation accuracy. The F values of the two study sites were all higher than 0.95 (Table III). The individual tree segmentation accuracy from UAV lidar data was relatively lower compared to that from backpack lidar data (Table III). The individual tree segmentation accuracy in site 2 was slightly higher than that of site 1, which might be caused by the fact that the canopy coverage in site 2 was much lower than that in site 1. Here, the displacement of tree locations was quantified by the difference in the distances between a pair of neighboring trees from different lidar datasets (Fig. 7). On average, there was an around 30 cm and 40 cm displacement in site 1 and site 2, respectively (Fig. 7b).

TABLE III
ACCURACY ASSESSMENT FOR THE INDIVIDUAL TREE SEGMENTATION RESULTS FROM THE BACKPACK AND UAV LIDAR DATA AT THE TWO STUDY SITES.

	Site 1		Site 2	
	Backpack	UAV	Backpack	UAV
TP	213	289	156	187
FN	10	49	4	9
FP	11	22	2	22
r	0.955	0.855	0.975	0.954
p	0.951	0.873	0.987	0.895
F	0.953	0.864	0.981	0.924

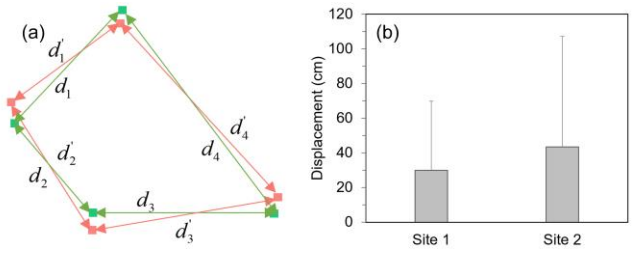

Fig. 7. (a) A schematic illustration of tree location displacement obtained from backpack and UAV lidar datasets, and (b) the average tree location displacements in site 1 and site 2. Red dots in (a) represent tree locations derived from backpack lidar data and green dots represent tree locations derived from UAV lidar data. d and d' represent the distance between two neighboring trees. The displacement in (b) was calculated as the horizontal distance difference of a pair of trees before the registration.

The TIN matching process identified 7 pairs of trees from site 1 and 11 pairs of trees from site 2, which were used to perform the coarse registration. The standard deviations of residuals between tree locations after coarse registration were 0.84 m and 0.93 m for site 1 and site 2, respectively. The two lidar datasets were closely aligned with each other following fine registration that the fused backpack UAV lidar point clouds in tandem provided more complete forest structural information than either platform alone (Fig. 8). and the horizontal error and vertical error after the fine registration step were 0.300 m and 0.146 m, respectively, for site 1, and were 0.211 m and 0.187 m, respectively, for site 2.

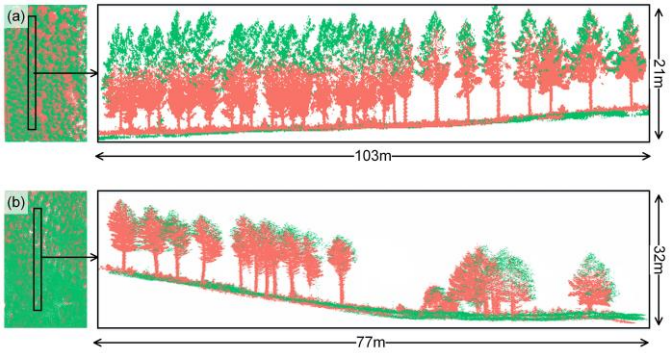

Fig. 8. Profiles of the registered backpack lidar data (red dots) and UAV lidar data (green points) in (a) site 1 and (b) site 2.

D. *Multi-scan TLS Data Registration Results*

The individual tree segmentation accuracy of the non-registered TLS data was more than 95% for all four scans (Table IV). After TIN matching, there were 11, 10 and 8 trees reserved to calculate the rotation matrix and translation vector for the coarse registration between the TLS data from scan position 1 and those from scan position 2-4, respectively. The standard deviation of residuals between tree locations after coarse registration between the TLS data from scan position 1 and those from scan position 2-4 was 0.161 m, 0.154 m and 0.157 m. The four TLS scans matched with each other very well after the fine registration (Fig. 9) and the standard deviation of residuals was 0.038 m, 0.050 m and 0.053 m, compared with a value of 0.013 m, 0.009 m and 0.011 m obtained by manual registration using the Riegl RiSCAN Pro software.

Table IV
ACCURACY ASSESSMENT FOR THE INDIVIDUAL TREE SEGMENTATION RESULTS FROM THE MULTI-SCAN TLS DATA

	Scan 1	Scan 2	Scan 3	Scan 4
TP	73	66	74	63
FN	1	2	3	1
FP	1	0	1	2
r	0.986	0.971	0.961	0.984
p	0.986	1.000	0.987	0.969
F	0.986	0.985	0.974	0.977

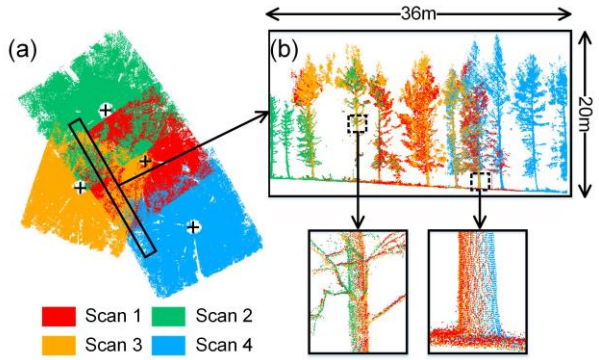

Fig. 9. (a) The final registration results of the four TLS scans on site 3 using the proposed framework; (b) a profile example of the registered TLS point cloud and enlarged examples of two tree segments in the profile. The black rectangle in (a) represents the extent of the profile and the "+" marks represent the scanning positions.

IV. DISCUSSION

Multi-platform lidar data registration is increasingly in demand in lidar forest applications. Through the fusion of multi-platform lidar data, it can overcome the limitations of single-platform/single-scan lidar data and allow for the more complete derivation of forest structure parameters [51]. However, due to the complexity and irregularity of forests and the often absent or inaccurate GPS positioning information, traditional point cloud registration methods can hardly be used in forest environments [52]. Recently, there have been successful attempts to develop marker free registration methods to increase the efficiency of multi-platform lidar data registration. Generally, these methods can be divided into two categories, i.e., looking for geometric features for registration inside the multi-platform lidar data (e.g., stem centers and stem curves) and looking for a globally optimized transformation solution based on lidar-derived tree attributes (e.g., tree height and DBH) [33-36]. The methods using geometric features inside the point clouds have a similar idea as the proposed framework, that is using the unique tree characteristics as the referencing features [33], [34]. However, compared with the proposed framework, these methods have disadvantages of less adaptability to different platforms. Currently, methods based on tree stem geometric features cannot be used in registrations involving top-view lidar data (e.g., UAV lidar data), because top-view lidar data cannot capture complete tree stem information. As to the methods using globally optimized transformation solution, they might not be achievable when the required tree attributes were inaccurate or missing. For example, the method proposed by Kelbe *et al.* [37] required accurate tree stem maps and DBH estimations, which can be hard to obtain from UAV lidar data [53]; and the method proposed by Polewski *et al.* [36] required a precondition that the Z axis of multi-platform lidar data should be well aligned or could be aligned by tree stem orientations, which can be hard to satisfy in complex forest environments due to the inaccurate GPS information under the forest canopy and the lack of trunk information in down-looking lidar platforms. The proposed registration framework only required tree locations to fuse

multi-platform lidar data, and does not require any exterior information to assist the registration process, which can largely improve the multi-platform lidar data registration applicability.

Overall, the proposed framework worked well in both experiments in this study. The fusion of backpack and UAV lidar datasets achieved vertical accuracy better than 20 cm and horizontal accuracy better than 30 cm on sites 1 and 2. Considering the positioning uncertainty within the backpack and UAV lidar data and the error propagation effect during the registration, the registration results should satisfy many forest-related applications. The horizontal displacement after registration for site 1 was much larger than that for site 2 (Fig. 8). The possible reason might be that the terrain in site 1 was much flatter than site 2. Since the differences in Z values in flat terrain were not obvious, the process of the ICP algorithm might lack features in the Z direction. In this case, the ICP algorithm may converge to a local optimum [54], [55], which therefore leads to larger horizontal errors. The accuracy of the registration of multi-scan TLS data was much higher than that for the registration of backpack and UAV lidar data. This indicates that the performance of the proposed framework might be improved by increasing the precision of lidar data. Although the registration accuracy of multi-scan TLS data registration is still lower than that of using a manual registration method based on referencing targets, it can be used as a preliminary step before performing manual registration to increase the efficiency. Future studies can consider using the referencing targets as exterior information to further improve the registration accuracy.

Individual tree segmentation is the prerequisite for the proposed registration framework, and the accuracy of individual tree segmentation might have a considerable influence on the registration accuracy. In this study, the side-view backpack lidar data can obtain rich tree trunk information, and the corresponding individual tree segmentation accuracy is much higher than UAV lidar data (Table III). Therefore, this study matched UAV lidar data to backpack lidar data to reduce the influence of incorrectly segmented trees. To further evaluate the influence of individual tree segmentation accuracy on the registration accuracy, we simulated a scenario where the individual tree segmentation accuracy was 100% and randomly removed/added errors from/to the UAV lidar segmentation results in site 1 to manipulate the values of *r* and *p* from UAV individual tree segmentation results, which were changed from 100% to 75% with a step of 5%. As can be seen in Fig. 10, with the decrease of *r* and *p*, the number of matched tree pairs also decreased. However, when *r* and *p* were both higher than 80%, there were enough matched tree pairs to perform the following coarse and fine registration steps. Currently, most individual tree segmentation practices from lidar can reach an overall accuracy higher than 85% [56], [57]. Therefore, we believe that the proposed framework can be used to register multi-platform lidar data effectively in most forest environments.

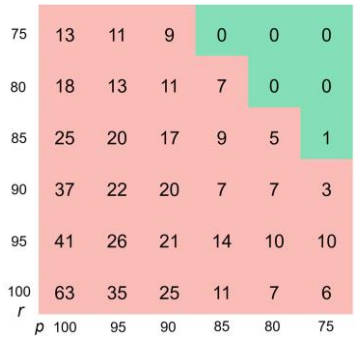

Fig. 10. The influence of individual tree segmentation accuracy on the TIN matching results. *r* and *p* represent the recall and precision, and each element in the matrix represents the number of matched tree pairs. Elements colored in red indicate that there are enough matched tree pairs for registration, and elements colored in green indicate that the number of matched tree pairs is insufficient for registration.

There are five user-defined parameters in the algorithm, as listed in Table II. T_S and T_I are two iteratively updated parameters, which can be assigned with relatively small values (around 0.75) to ensure that the TIN matching process can find enough tree pairs. T_{VS} is a *VS* threshold, which can be determined by a simple trial-and-error process. The number of matched tree pairs should be monitored in the trial-and-error process. The larger the T_{VS} is, the fewer the number of matched tree pairs is. Since solving the rotation matrix and translation vector only requires three paired targets [58], [59], the registration process can be conducted once the trial-and-error process finds three matched tree pairs. However, the robustness of the transformation solution can be improved by introducing more referencing targets [58-60]. Therefore, we encourage users to continue the trial-and-error process with as many matched tree pairs (> 8 pairs) as possible. T_N determines the number of iterations, which can be set to a relatively large number to eliminate the "one-to-many" phenomenon in the TIN matching process. In summary, the above four parameters can either be determined by a simple trial-and-error process or do not have a significant influence on the registration framework. The only parameter that cannot be easily obtained and might have a significant influence on the registration accuracy is *NN*. To assess the sensitivity of the proposed framework to *NN*, we iteratively increased *NN* and ran the registration processes for site 1 repeatedly. To eliminate the influence of individual tree segmentation error on the results, the registration processes were running under a simulated scenario where the individual tree segmentation accuracy was 100%. All other parameters were set the same as Table II. Since T_{VS} was set to five and at least seven points were needed to build a TIN with five triangles, the number of matched tree pairs would be zero if $NN \leq 7$. Therefore, *NN* was increased from 8 to 15 with a step size of one in this analysis. As can be seen in Fig. 11, with the increase of *NN*, the number of matched tree pairs first increased and then decreased, and the largest value appeared when *NN* was 11. The difference in the number of matched tree pairs was less than 10 when NN was set between 10 and 12. Considering the redundant information provided by a large number of matched tree pairs for registration, it should be a safe choice to set *NN* as around twice the value of T_{VS}.

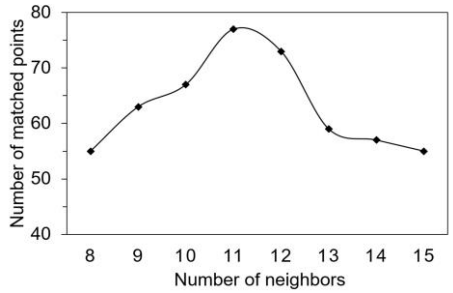

Fig. 11. The influence of the number of neighbors (*NN*) on the TIN matching results on site 1.

Although the proposed framework shows great potential in solving the bottleneck of multi-platform lidar data registration in forest environments, it still has limitations which need to be addressed in future studies. Firstly, the proposed framework might not work well in regularly planted forests, because the regular arrangement of stems will likely result in very similar TINs built from different tree locations. Using exterior information to assist the proposed framework (such as referencing targets) might be a solution to this issue. Moreover, the present study only tested the proposed framework in very limited forest environments. Further studies are still needed to investigate how the framework performs in other more complex forest environments, such as deciduous forests. In dense deciduous forests, the tightly interlocked canopies might cause low accuracy of individual tree segmentation from UAV lidar data. Using areas around forest gaps with sparse tree distribution instead of the whole study area might be beneficial to increase the registration accuracy.

V. Conclusions

This study proposes an automatic point cloud registration framework for multi-platform lidar data fusion in forest environments. Based on the assumption that each forest stand has a unique spatial distribution of trees, the proposed framework identifies tree pairs from multi-platform lidar data by a TIN matching strategy. The identified tree pairs are then used to coarsely match the target point cloud to the source point cloud, and the final registration result could be obtained by running an ICP-based fine registration process. The proposed framework was tested to register backpack lidar data and UAV lidar data and register multi-scan TLS data. Overall, the proposed framework achieved satisfying accuracies in both experiments. The vertical error of the registration between backpack and UAV lidar data was less than 20 cm for both study sites, and horizontal error was less than 30 cm. The registration error was much lower for the fusion of multi-scan TLS data. The average registration error was about 4.7 cm. Individual tree segmentation errors can reduce the number of matched tree points. However, as long as the number of matched tree points was enough for solving the rotation matrix and translation vector, the increase of tree segmentation errors (<20%) did not have significant influence on the registration accuracy. Moreover, the proposed framework was not overly sensitive to the settings of user-defined parameters. All parameters can be easily calculated or obtained by a simple trial-and-error process.

References

[1] H. Latifi, F. E. Fassnacht, J. Müller, A. Tharani, S. Dech, and M. Heurich, "Forest inventories by LiDAR data: A comparison of single tree segmentation and metric-based methods for inventories of a heterogeneous temperate forest," *Int. J. Appl. Earth Obs. Geoinformation*, vol. 42, pp. 162–174, 2015.

[2] M. Bouvier, S. Durrieu, R. A. Fournier, and J. P. Renaud, "Generalizing predictive models of forest inventory attributes using an area-based approach with airborne LiDAR data," *Remote Sens. Environ.*, vol. 156, pp. 322–334, 2015.

[3] S. Saarela *et al.*, "Model-assisted estimation of growing stock volume using different combinations of LiDAR and Landsat data as auxiliary information," *Remote Sens. Environ.*, vol. 158, pp. 431–440, 2015.

[4] A. E. L. Stovall, A. G. Vorster, R. S. Anderson, P. H. Evangelista, and H. H. Shugart, "Non-destructive aboveground biomass estimation of coniferous trees using terrestrial LiDAR," *Remote Sens. Environ.*, vol. 200, pp. 31–42, 2017.

[5] F. Morsdorf, E. Meier, B. Kötz, K. I. Itten, M. Dobbertin, and B. Allgöwer, "LIDAR-based geometric reconstruction of boreal type forest stands at single tree level for forest and wildland fire management," *Remote Sens. Environ.*, vol. 92, no. 3, pp. 353–362, 2004.

[6] M. A. Wulder, C. W. Bater, N. C. Coops, T. Hilker, and J. C. White, "The role of LiDAR in sustainable forest management," *For. Chron.*, vol. 84, no. 6, pp. 807–826, 2008.

[7] Q. Ma, T. Hu, Y. Su, Q. Guo, J. J. Battles, and M. Kelly, "Individual tree level forest fire assessment using bi-temporal LIDAR data," in *IGARSS 2018-2018 IEEE International Geoscience and Remote Sensing Symposium*, 2018, pp. 4308–4311.

[8] X. Liang, J. Hyyppä, A. Kukko, H. Kaartinen, A. Jaakkola, and X. Yu, "The use of a mobile laser scanning system for mapping large forest plots," *IEEE Geosci. Remote Sens. Lett.*, vol. 11, no. 9, pp. 1504–1508, 2014.

[9] X. Liang *et al.*, "Terrestrial laser scanning in forest inventories," Isprs *J. Photogramm. Remote Sens.*, vol. 115, pp. 63–77, 2016.

[10] L. Wallace, A. Lucieer, Z. Malenovskỳ, D. Turner, and P. Vopěnka, "Assessment of forest structure using two UAV techniques: A comparison of airborne laser scanning and structure from motion (SfM) point clouds," *Forests*, vol. 7, no. 3, p. 62, 2016.

[11] Y. Su, H. Guan, T. Hu, and Q. Guo, "The integration of uavand backpack lidar systems for forest inventory," in *IGARSS 2018-2018 IEEE International Geoscience and Remote Sensing Symposium*, 2018, pp. 8757–8760.

[12] C. Paris, D. Valduga, and L. Bruzzone, "A Hierarchical Approach to Three-Dimensional Segmentation of LiDAR Data at Single-Tree Level in a Multilayered Forest," *IEEE Trans. Geosci. Remote Sens.*, vol. 54, no. 7, pp. 4190–4203, 2016.

[13] T. Hilker *et al.*, "Comparison of terrestrial and airborne LiDAR in describing stand structure of a thinned lodgepole pine forest," *J. For.*, vol. 110, no. 2, pp. 97-104(8), 2012.

[14] P. W. Theiler, J. D. Wegner, and K. Schindler, "Globally consistent registration of terrestrial laser scans via graph optimization," *Isprs J. Photogramm. Remote Sens.*, vol. 109, pp. 126–138, 2015.

[15] L. Yan, J. Tan, H. Liu, H. Xie, and C. Chen, "Automatic registration of TLS-TLS and TLS-MLS point clouds using a genetic algorithm," *Sensors*, vol. 17, no. 9, 2017.

[16] L. Cheng *et al.*, "Registration of Laser Scanning Point Clouds: A Review," *Sensors*, vol. 18, no. 5, p. 1641, 2018.

[17] Z. Dong, B. Yang, F. Liang, R. Huang, and S. Scherer, "Hierarchical registration of unordered TLS point clouds based on binary shape context descriptor," Isprs *J. Photogramm. Remote Sens.*, vol. 144, pp. 61–79, 2018.

[18] B. Morago, G. Bui, T. Le, N. H. Maerz, and Y. Duan, "Photograph lidar registration methodology for rock discontinuity measurement," *IEEE Geosci. Remote Sens. Lett.*, vol. PP, no. 99, pp. 1–5, 2018.

[19] I. Klein and S. Filin, "Lidar and INS fusion in periods of GPS outages for mobile laser scanning mapping systems," Isprs - *Int. Arch. Photogramm. Remote Sens. Spat. Inf. Sci.*, vol. XXXVIII-5/W12, no. 5, pp. 231–236, 2012.

[20] L. Zhu and R. Shi, “Research on target accuracy for ground-based lidar,” in *Laser Radar Technology and Applications XIV*, 2009, vol. 7323, p. 73230K.
[21] H. Cho, S. Hong, S. Kim, H. Park, I. Park, and H. G. Sohn, “Application of a terrestrial LIDAR system for elevation mapping in Terra Nova Bay, Antarctica,” *Sensors*, vol. 15, no. 9, pp. 23514–23535, 2015.
[22] A. Wendt, “A concept for feature based data registration by simultaneous consideration of laser scanner data and photogrammetric images,” *Isprs J. Photogramm. Remote Sens.*, vol. 62, no. 2, pp. 122–134, 2007.
[23] B. O. Abayowa, A. Yilmaz, and R. C. Hardie, “Automatic registration of optical aerial imagery to a LiDAR point cloud for generation of city models,” Isprs *J. Photogramm. Remote Sens.*, vol. 106, pp. 68–81, 2015.
[24] L. Cheng *et al.*, “A symmetry-based method for Lidar point registration,” *IEEE J. Sel. Top. Appl. Earth Obs. Remote Sens.*, vol. 11, no. 1, pp. 285–299, 2018.
[25] S. Rusinkiewicz and M. Levoy, “Efficient Variants of the ICP Algorithm,” *Proc. 3DIM*, pp. 145–152, 2001.
[26] A. Gressin, C. Mallet, J. Demantké, and N. David, “Towards 3D lidar point cloud registration improvement using optimal neighborhood knowledge,” Isprs *J. Photogramm. Remote Sens.*, vol. 79, no. I–3, pp. 240–251, 2013.
[27] A. R. G. Large, G. L. Heritage, and M. E. Charlton, *Laser Scanning: The Future*. Wiley-Blackwell, 2009.
[28] K. E. Anderson *et al.*, “Estimating vegetation biomass and cover across large plots in shrub and grass dominated drylands using terrestrial lidar and machine learning,” *Ecol. Indic.*, vol. 84, pp. 793–802, 2018.
[29] C. Brenner, C. Dold, and N. Ripperda, “Coarse orientation of terrestrial laser scans in urban environments,” *Isprs J. Photogramm. Remote Sens.*, vol. 63, no. 1, pp. 4–18, 2008.
[30] Jen, JerJaw and Tzu, YiChuang, “Registration of ground-based LiDAR point clouds by means of 3D line features,” *J. Chin. Inst. Eng.*, vol. 31, no. 6, pp. 1031–1045, 2008.
[31] A. Gruen and D. Akca, “Least squares 3D surface and curve matching,” *Isprs J. Photogramm. Remote Sens.*, vol. 59, no. 3, pp. 151–174, 2005.
[32] X. Ge and T. Wunderlich, “Surface-based matching of 3D point clouds with variable coordinates in source and target system,” *Isprs J. Photogramm. Remote Sens.*, vol. 111, pp. 1–12, 2016.
[33] J. G. Henning and P. J. Radtke, “Multiview range-image registration for forested scenes using explicitly-matched tie points estimated from natural surfaces,” *Isprs J. Photogramm. Remote Sens.*, vol. 63, no. 1, pp. 68–83, 2008.
[34] J. Liu et al., “Automated matching of multiple terrestrial laser scans for stem mapping without the use of artificial references,” *Int. J. Appl. Earth Obs. Geoinformation*, vol. 56, pp. 13–23, 2017.
[35] D. Kelbe, J. van Aardt, P. Romanczyk, M. van Leeuwen, and K. Cawse-Nicholson, “Marker-gree registration of forest terrestrial laser scanner data pairs with embedded confidence metrics,” *IEEE Trans. Geosci. Remote Sens.*, vol. 54, no. 7, pp. 4314–4330, Jul. 2016.
[36] P. Polewski, W. Yao, L. Cao, and S. Gao, “Marker-free coregistration of UAV and backpack LiDAR point clouds in forested areas,” *Isprs J. Photogramm. Remote Sens.*, vol. 147, pp. 307–318, Jan. 2019.
[37] J. Mustonen, P. Packalén, and A. Kangas, “Automatic segmentation of forest stands using a canopy height model and aerial photography,” *Scand. J. For. Res.*, vol. 23, no. 6, pp. 534–545, 2008.
[38] L. Jing, B. Hu, J. Li, and T. Noland, “Automated delineation of individual tree crowns from lidar data by multi-scale analysis and segmentation,” *Photogramm. Eng. Remote Sens.*, vol. 78, no. 12, pp. 1275–1284, 2012.
[39] A. Khosravipour, A. K. Skidmore, M. Isenburg, T. Wang, and Y. A. Hussin, “Generating pit-free canopy height models from airborne Lidar,” *Photogramm. Eng. Remote Sens.*, vol. 80, no. 9, pp. 863–872, 2014.
[40] W. Li, Q. Guo, M. K. Jakubowski, and M. Kelly, “A new method for segmenting individual trees from the lidar point cloud,” *Photogramm. Eng. Remote Sens.*, vol. 78, no. 1, pp. 75–84, 2012.
[41] X. Lu, Q. Guo, W. Li, and J. Flanagan, “A bottom-up approach to segment individual deciduous trees using leaf-off lidar point cloud data,” Isprs *J. Photogramm. Remote Sens.*, vol. 94, pp. 1–12, 2014.
[42] S. Tao *et al.*, “Segmenting tree crowns from terrestrial and mobile LiDAR data by exploring ecological theories,” Isprs *J. Photogramm. Remote Sens.*, vol. 110, pp. 66–76, 2015.
[43] M. K. Jakubowski, W. Li, Q. Guo, and M. Kelly, “Delineating individual trees from LiDAR data: A comparison of vector-and raster-based segmentation approaches,” *Remote Sens.*, vol. 5, no. 9, pp. 4163–4186, 2013.
[44] Victorj. D. Tsai, “Delaunay triangulations in TIN creation: an overview and a linear-time algorithm,” *Int. J. Geogr. Inf. Syst.*, vol. 7, no. 6, pp. 501–524, 1993.
[45] D. Zhou, G. Li, and Y. Liu, “Effective corner matching based on Delaunay triangulation,” in *IEEE International Conference on Robotics and Automation, 2004. Proceedings. ICRA’04. 2004*, 2004, vol. 3, pp. 2730–2733.
[46] O. Chum, J. Matas, and J. Kittler, “Locally Optimized RANSAC,” *Lect. Notes Comput. Sci.*, vol. 2781, pp. 236–243, 2003.
[47] T. Fei, X. H. Liang, Z. Y. He, and G. L. Hua, “A registration method based on nature feature with klt tracking algorithm for wearable computers,” in *International Conference on Cyberworlds*, 2009.
[48] N. Li, P. Cheng, M. A. Sutton, and S. R. Mcneill, “Three-dimensional point cloud registration by matching surface features with relaxation labeling method,” *Exp. Mech.*, vol. 45, no. 1, pp. 71–82, 2005.
[49] G. C. Sharp, W. L. Sang, and D. K. Wehe, “ICP registration using invariant features,” *IEEE Trans Pami*, vol. 24, no. 1, pp. 90–102, 2002.
[50] X. Zhao, Q. Guo, Y. Su, and B. Xue, “Improved progressive TIN densification filtering algorithm for airborne LiDAR data in forested areas,” *Isprs J. Photogramm. Remote Sens.*, vol. 117, pp. 79–91, 2016.
[51] M. Hämmerle *et al.*, “Simulating various terrestrial and uav lidar scanning configurations for understory forest structure modelling,” *Isprs Annals of Photogrammetry, Remote Sensing & Spatial Information Sciences*, vol. 4, 2017.
[52] W. Zhang, Y. Chen, H. Wang, M. Chen, X. Wang, and G. Yan, “Efficient registration of terrestrial LiDAR scans using a coarse-to-fine strategy for forestry applications,” *Agric. For. Meteorol.*, vol. 225, pp. 8–23, 2016.
[53] R. A. Chisholm, J. Cui, S. K. Lum, and B. M. Chen, “UAV LiDAR for below-canopy forest surveys,” *J. Unmanned Veh. Syst.*, vol. 1, no. 01, pp. 61–68, 2013.
[54] Y.-J. Lee and J.-B. Song, “Three-dimensional iterative closest point-based outdoor SLAM using terrain classification,” *Intell. Serv. Robot.*, vol. 4, no. 2, pp. 147–158, 2011.
[55] Y.-J. Lee, Y.-H. Ji, J.-B. Song, and S.-H. Joo, “Performance improvement of ICP-based outdoor SLAM using terrain classification,” in *international conference on advanced mechatronics: toward evolutionary fusion of IT and mechatronics: ICAM.*, 2010, pp. 243–246.
[56] G. PriedītIs, I. Šmits, S. DaģIs, D. Dubrovskis, S. Treija, and I. Skuja, “Individual tree identification using combined LiDAR data and optical imagery.,” in *International Scientific Conference Proceedings, “research for Rural Development”, Jelgava, Latvia, 16-18 May*, 2012.
[57] E. Ayrey *et al.*, “Layer Stacking: A Novel Algorithm for Individual Forest Tree Segmentation from LiDAR Point Clouds,” *Can. J. Remote Sens.*, vol. 43, no. 1, pp. 16–27, 2017.
[58] L. Quan, “Self-calibration of an affine camera from multiple views,” Int. J. Comput. Vis., vol. 19, no. 1, pp. 93–105, 1996.
[59] C.-P. Lu, G. D. Hager, and E. Mjolsness, “Fast and globally convergent pose estimation from video images,” *IEEE Trans. Pattern Anal. Mach. Intell.*, vol. 22, no. 6, pp. 610–622, 2000.
[60] R. I. Hartley, “In defence of the 8-point algorithm,” in *Proceedings of IEEE international conference on computer vision*, 1995, pp. 1064–1070.

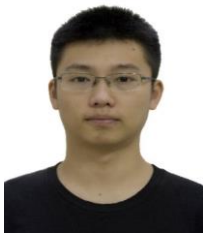

Hongcan Guan received a B.S. degree in remote sensing science and technology from Wuhan University, Wuhan, China, in 2014, and a M.S. degree in electronics and communication engineering from the Institute of Opto-electronics, Chinese Academy of Sciences, Beijing, China, in 2017.
He is a Ph.D. student in the Institute of Botany, Chinese Academy of Sciences, Beijing. His research focuses on using remote sensing technology to solve vegetation mapping related challenges.

Yanjun Su received a B.E. degree in surveying and mapping engineering from China University of Geosciences, Beijing, China, in 2009, a M.S. degree in geographic information science from the institute of Geographic Sciences and Natural Resources Research, Chinese Academy of Sciences, Beijing, in 2012, and a Ph.D. degree in environmental systems from the University of California at Merced, Merced, CA, USA, in 2017.
He is an associate professor in the Institute of Botany, Chinese Academy of Sciences, Beijing. His research focuses on applying geographic information science and remote sensing to understand the influence of anthropogenic activities and global climate change on terrestrial ecosystems, with a particular emphasis on the terrestrial carbon cycle, terrestrial biodiversity, energy balance and land-use/land-cover change.

Tianyu Hu received a B.S. degree in ecology from China Agriculture University, Beijing, China, in 2008, and a Ph.D. degree in Institute of Botany, Chinese Academy of Sciences, Beijing, in 2014.
He is an assistant professor in the Institute of Botany, Chinese Academy of Sciences, Beijing. His research focuses on using LiDAR technology and dynamic vegetation model to understand forest ecosystem, especially in forest structure, function and biodiversity.

Rui Wang received a B.S. degree in forestry from Huazhong Agricultural University, Wuhan, China, in 2016.
She is a master student in the Institute of Botany, Chinese Academy of Sciences, Beijing, China. Her research focuses on exploring the application of lidar technology in forest inventory.

Qin Ma received a B.S. degree in forestry from Huazhong Agricultural University, Wuhan, China, in 2017.
She is a Ph.D. student in the Institute of Botany, Chinese Academy of Sciences, Beijing, China. Her research focuses on using LiDAR technology to assess biodiversity.

Qiuli Yang received a B.S. degree in geographic information system from Xinjiang Agricultural University and a M.S. degree in geography from Xinjiang University, Xinjiang, China, in 2014 and 2018, respectively.
She is a Ph.D. student in the Institute of Botany, Chinese Academy of Sciences, Beijing, China. Her research focuses on using multi-source remote sensing data to derive forest structural parameters and functional parameters.

Xiliang Sun received a B.S. degree in remote sensing from the Information Engineering University, Zhengzhou, China, in 2010, and a M.S. degree in photogrammetry and remote sensing from Shandong University of Science and Technology, Qingdao, China, in 2013.
He is an engineer in the Institute of Botany, Chinese Academy of Sciences, Beijing, China. His recent research areas include LiDAR algorithm development and its applications in city ecology, such as point clouds segmentation, city green biomass extraction and 3-D modeling.

Yumei Li received the B.S. degree in ecology from Hebei Agricultural University, Baoding, China, in 2012, and the Ph.D. degree from the Institute of Botany, Chinese Academy of Sciences, Beijing, China, in 2018.
She is currently a post-doctor in the Institute of Botany, Chinese Academy of Sciences, Beijing. Her current research interests include the studies on retrieval method of structural and biophysical parameters of vegetation using light detection and ranging (LiDAR) data and using remote sensing technology to answer key scientific issues on ecological science.

Shichao Jin received a B.S. degree in forestry from Huazhong Agricultural University, Wuhan, China, in 2016.
He is a Ph.D. student in the Institute of Botany, Chinese Academy of Sciences, Beijing, China. His research focuses on using deep learning and LiDAR technology to solve phenotyping related challenges.

Zhang Jing received a B.S. degree in landscape architecture from Sichuan University.
She is a master student in the Institute of Botany, Chinese Academy of Sciences, Beijing. Her research focuses on exploring the application of lidar technology in urban planning.

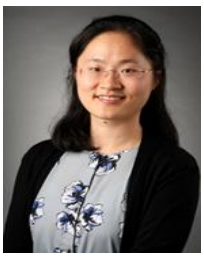

Qin Ma received a B.S. degree in geography from Nanjing University, Nanjing, China in 2011; a M.S. degree in geography from Western University, Ontario, Canada in 2013, and a Ph.D. degree in environmental Systems from the University of California, Merced, USA in 2018.
She is an assistant professor in the Department of Forestry, Mississippi State University. Her research focuses on using remote sensing and spatial techniques to map, monitor, and model vegetation structural and functional changes in response to human activities and climate change.

Min Liu received a B.S. degree in agronomy from Henan Agricultural University, in 1994, and a M.S. degree in science of public management and a Ph.D. degree in agricultural economics from Renmin University, Beijing, China, in 2002 and 2009, respectively.
He is a senior researcher in Forestry and Economics and Development Research Center of National Forestry and Grassland Administration, Beijing. His recent research areas focus on natural resources and environmental economics, green economy and sustainable development.

Fayun Wu received a B.S. degree in soil and water conservation from Beijing Forestry University, Beijing, China, in 1998, and a M.S. degree in forest management from Beijing Forestry University in 2002, Beijing.
He is a senior engineer in Academy of Inventory and Planning of National Forestry and Grassland Administration, Beijing. His recent research areas focus on remote sensing applications in forestry.

Qinghua Guo received a B.S. degree in environmental science and a M.S. degree in remote sensing and geographic information system (GIS) from Peking University, Beijing, China, in 1996 and 1999, respectively, and received a Ph.D. degree in environmental science from the University of California, Berkeley, CA, USA, in 2005.
He is a professor in the Institute of Botany, Chinese Academy of Sciences, Beijing. He is also an adjunct professor and a member of the founding faculty in the School of Engineering, University of California at Merced, Merced, CA, USA. His recent research areas include GIS and remote sensing algorithm development and their environmental applications, such as object-based image analysis, geographic one-class data analysis, and LiDAR data processing.